

Development of a Continuous Photochemical Bromination/Alkylation Sequence En Route to AMG 423

Kyle Quasdorf,* James I. Murray, Hanh Nguyen, Maria V. Silva Elipe, Ari Ericson, Eric Kircher, Lianxiu Guan, and Seb Caille



Cite This: *Org. Process Res. Dev.* 2022, 26, 458–466



Read Online

ACCESS |



Metrics & More



Article Recommendations



Supporting Information

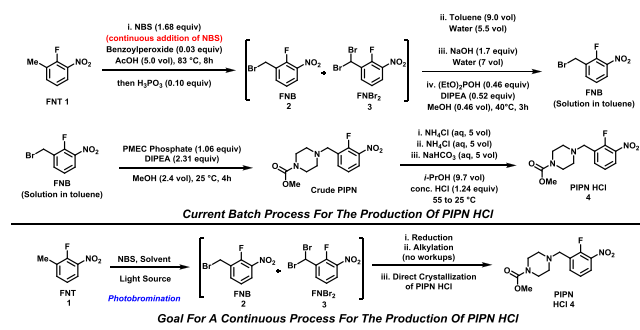
ABSTRACT: The development of a photochemical bromination/alkylation sequence as part of a continuous process for the synthesis of an intermediate en route to AMG 423 is discussed. Highlights of this continuous process include a significant reduction in reaction time and the elimination of aqueous waste streams. Also discussed are mechanistic and kinetic studies offering insights into notable features of the photochemical bromination.

KEYWORDS: *photochemistry, Wohl–Ziegler, kinetics, photobromination, continuous manufacturing*

INTRODUCTION

The Wohl–Ziegler reaction has been a staple in organic synthesis over the last century for the allylic and benzylic bromination of compounds.¹ Our group has recently reported on the optimization and kinetic studies that have allowed for the successful implementation of this reaction on the manufacturing scale as part of the process for the production of AMG 423.^{2,3} In order to facilitate further streamlining and the optimization of the process, we sought to develop a second-generation route utilizing a photochemical bromination as part of a fully telescoped continuous process for the conversion of fluoro-nitrotoluene (FNT) **1** to piperazine nitrotoluene hydrochloride salt (PIPn HCl) **4**, as shown in Scheme 1. We believe that this would offer process

Scheme 1. Current Batch Process of the Production of PIPn HCl (Top) and the Proposed Second-Generation Approach (Bottom)



improvements in several areas including (1) the removal of the need for benzoyl peroxide as the chemical initiator, which was responsible for low-level impurities in the batch process, (2) the elimination of all aqueous workups to streamline the process and minimize waste output, and (3) allow for improved reaction times with regard to the bromination.

We were inspired to take this approach by the elegant work reported by numerous research groups in the past decade for conducting the Wohl–Ziegler reaction using readily available and light-emitting diodes (LEDs) or compact fluorescent lamps (CFLs), thus eliminating the need for using harsh ultraviolet (UV) lamps or chemical initiators in this reaction.^{4,5} Other important considerations for successfully implementing this type of reaction in a continuous flow setup have also been reported in the literature.⁶

RESULTS AND DISCUSSION

Bromination Optimization. We began our reaction development for the bromination of **1** by examining several reaction parameters, as highlighted in Table 1. Acetonitrile was identified as a promising reaction solvent, as demonstrated by previous reports,^{4a,b} offering good solubility for *N*-bromosuccinimide (NBS) as well as being a water-miscible solvent to allow for direct isolation by the addition of aqueous acid at the end of the process. NBS was explored as the most preferred brominating reagent, given its use in the existing process. Reaction screening was conducted using a commercially available microphotochemical reactor kit.⁷

We were pleased to find that under our initial conditions tested (Table 1, entries 1–3), good conversion of **1** to monobromide (FNB) **2** and dibromide (FNBBr₂) **3** was observed in approximately 6 h, resulting in an end of reaction composition that was very comparable to the chemically initiated bromination process. Given our aim of developing a continuous flow process, we then sought to further develop the

Received: December 10, 2021

Published: February 1, 2022

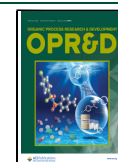


Table 1. Optimization of Conditions for the Bromination of 1

entry	solvent (0.530 M)	brominating reagent (equiv)	temperature ^a	time (min)	additive (equiv)	yield 2 (FNB) ^b	yield 3 (FNB ₂) ^b	yield 1 (FNT) ^b
1	CH ₃ CN	NBS (1.0)	25–30 °C	360	none	75	6	14
2	CH ₃ CN	NBS (1.25)	25–30 °C	360	none	78	9	8
3	CH ₃ CN	NBS (1.50)	25–30 °C	360	none	75	15	2
4	CH ₃ CN ^c	NBS (1.50)	25–30 °C	360	none	0	0	100
5	CH ₃ CN:AcOH (1:1)	NBS (1.0)	25–30 °C	180	none	79	10	9
6	CH ₃ CN:AcOH (1:1)	NBS (1.25)	25–30 °C	180	none	73	21	2
7	CH ₃ CN:AcOH (1:1)	NBS (1.50)	25–30 °C	180	none	53	41	0
8	CH ₃ CN	Bromine (1.25)	25–30 °C	360	none	<1	0	99
9	CH ₃ CN	NBS (1.0)	25–30 °C	180	bromine (0.25)	80	6	19
10	CH ₃ CN	DBDMH (0.6) ^d	25–30 °C	360	none	81	7	13
11	CH ₃ CN:AcOH (1:1)	DBDMH (0.6) ^d	25–30 °C	180	none	81	13	6
12	CH ₃ CN:TFA (1:1)	NBS (1.25)	25–30 °C	180	none	68	22	3
13	CH ₃ CN	NBS (1.25)	25–30 °C	60	TFA (1.0)	80	18	2
14	CH ₃ CN	NBS (1.25)	25–30 °C	60	TFA (5.0)	76	20	2
15	CH ₃ CN	NBS (1.25)	25–30 °C	60	AcOH (1.0)	54	2	43
16	CH ₃ CN	NBS (1.25)	25–30 °C	60	AcOH (5.0)	68	3	27
17	CH ₃ CN	NBS (1.25)	40 °C	25	TFA (1.0)	81	18	2
18	CH ₃ CN	NBS (1.25)	60 °C	15	TFA (1.0)	78	19	3
19	CH ₃ CN	NBS (1.25)	80 °C	10	TFA (1.0)	83	22	4
20	CH ₃ CN	NBS (1.25)	80 °C	15	TFA (0.25)	83	18	5

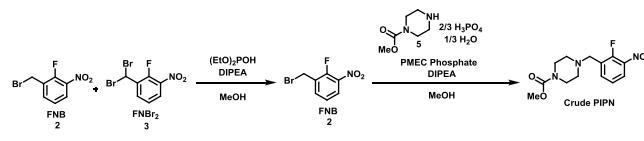
^aReactions conducted close to room temperature had slight variations because of the heat output from LEDs. ^bAssay yields determined by HPLC.

^cControl experiment run without exposure to 435–455 nm LED light. ^dDBDMH = 1,3-dibromo-5,5-dimethylhydantoin.

reaction conditions to allow for the completion of the bromination in minimal time. The use of AcOH as a cosolvent in these reactions has been previously noted to accelerate reaction rates.^{4b} Indeed, when employing a 1:1 mixture of CH₃CN:AcOH as the solvent, a noticeable rate enhancement was observed, allowing for reaction completion to be reached in 3 h (entries 5–7) with 1.25 equiv of NBS. Alternative brominating reagents were also examined. Bromine proved to be ineffective with <1% product seen after 6 h; however, NBS in combination with lower amounts of bromine leads to increased reaction rates (entries 8–9). The use of 1,3-dibromo-5,5-dimethylhydantoin (DBDMH) as the brominating reagent gave similar results to NBS, and the same solvent effects of increased reaction rate with AcOH as a cosolvent were observed (entries 10–11). The use of trifluoroacetic acid (TFA) as a cosolvent also proved viable, and in contrast to AcOH, the amount of TFA could be lowered to stoichiometric quantities, while still maintaining the same rate enhancement effect (entries 13–16) with reactions reaching completion in 60 min. Finally, increasing the reaction temperature provided clean conversion of 1 to 2 and 3 in only 15 min with the use of 0.25 equiv of TFA (entries 17–20). We reasoned that a reaction time of 15 min would be adequate for a continuous flow setup and then began the optimization of the subsequent downstream steps.

Reduction and Alkylation Optimization. With the conditions for successful bromination in hand, we turned our attention toward the reduction of dibromide 3 to monobromide 2, followed by the alkylation of 2 with piperazine methyl carbamate derivative (PMEC) 5 to generate crude streams of PIPN for isolation (Scheme 2).

Scheme 2. Downstream Steps of the Telescoped Process



From our previous experience with this reduction/alkylation sequence, we had utilized diethylphosphite as a mild reducing agent for selectively converting dibromide 3 to monobromide 2.³ Again, with the goal of minimizing the reaction time in mind, we were able to quickly adapt to these previous batch conditions to the ones that would be conducive to a continuous setup. Upon treatment with 0.40 equiv of diethylphosphite and 0.65 equiv of *N,N*-diisopropylethylamine (DIPEA) in MeOH at 50 °C, reaction streams of the composition as described in Table 1, entry 20, underwent smooth conversion of 3 → 2 in only 10 min with <1% of 3 remaining at the end of reaction and 90% assay yield of 2. Reactions conducted at 25 °C were sluggish and those conducted at 80 °C showed elevated levels of decomposition products. Alkylation of the reduction reaction stream was found to occur readily in 10 min with the addition of 1 equiv PMEC phosphate 5 and 2.5 equiv DIPEA in MeOH at 60 °C, furnishing a crude mixture of PIPN in 85% assay yield from 1 over the three steps. Crystallization of the crude PIPN stream could be readily achieved by the addition of either 4 M HCl in dioxane or concentrated aqueous HCl. However, further characterization of PIPN salts isolated in this manner by chloride ion analysis and X-ray powder diffraction (XRPD) revealed that it was in fact a mixture of the HCl and HBr salts. Process modifications for the selective isolation of the HCl salt

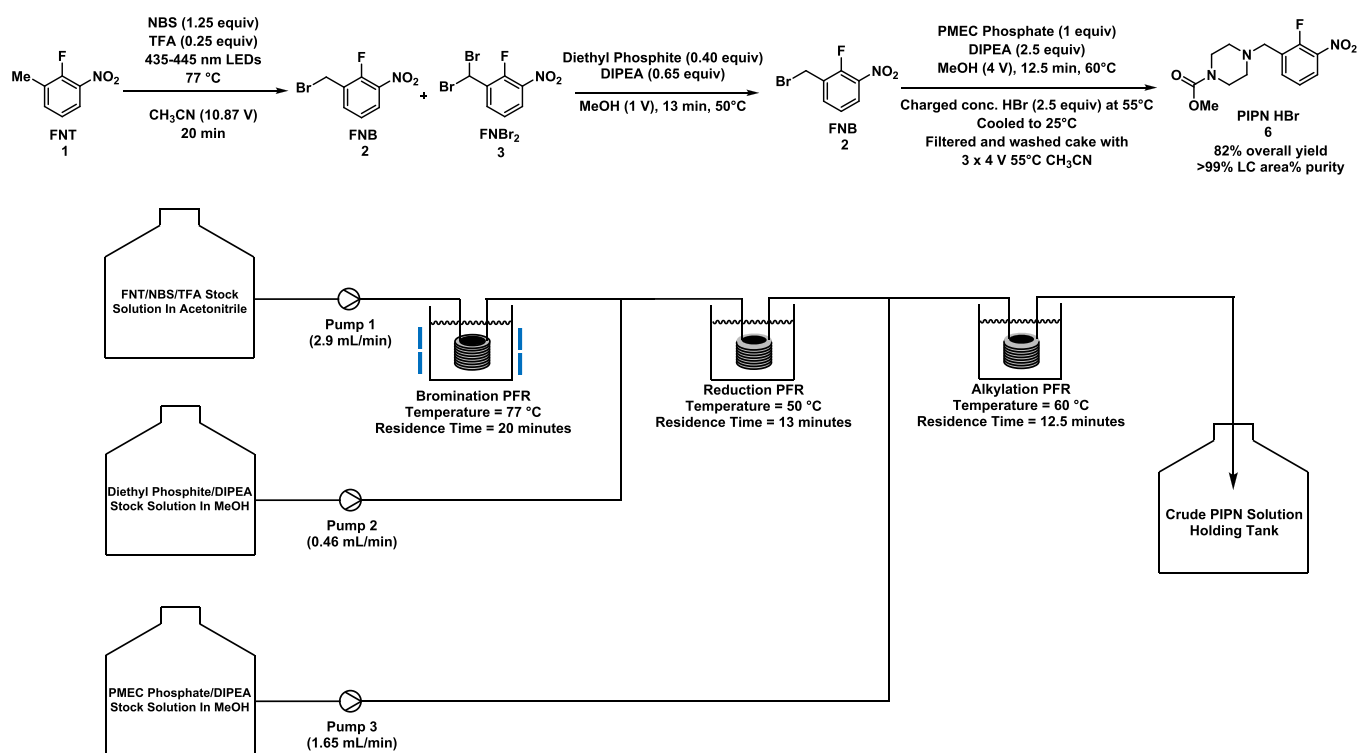


Figure 1. Schematic of a continuous setup for crude PIPN production.

under these telescoped reaction conditions proved ineffective, and thus, for this second-generation process, we targeted the isolation of PIPN as the HBr salt. Gratifyingly, the crystallization of the PIPN HBr salt could be achieved by the addition of concentrated HBr to crude PIPN streams.⁸ Having successfully developed and characterized the reaction profiles for each step in batch, we sought to translate this to a fully continuous flow process. This is in line with an overarching goal within our group to develop robust continuous processes, thus allowing for agile and innovative approaches to support the evolving needs of our pipeline, as highlighted in recent work on programs such as Carfilzomib,⁹ AMG 176,¹⁰ and AMG 397.¹¹

Development of a Continuous Flow Process for Crude PIPN. Given the short reaction times obtained from our optimization work in batch, we reasoned that a series of plug flow reactors (PFRs) would be ideal for a continuous flow process. A proof of principle set of experiments was conducted in small-scale Teflon-coiled tube microreactors.¹² In this way, each reaction could be rapidly explored in order to validate the results observed in batch. We were pleased to find that indeed the reaction times that we observed in batch translated to the corresponding residence times in the PFRs, and the crude PIPN streams produced with the series of microreactor PFRs were of the same composition as those from the batch.

With a successful demonstration of the small-scale continuous process, a larger laboratory-scale version was conducted. The conditions for each step as well as a schematic detail of the continuous setup are outlined in Figure 1.¹³ As shown, a solution of 1, NBS, and TFA was prepared in acetonitrile, and this was then pumped through the first PFR under irradiation from 435–445 nm LEDs at 77 °C with a residence time of 20 min.¹⁴ Clean conversion to the expected mixture of 2 and 3 occurred, and this stream was joined together at a mixing T-joint with a solution of diethylphosphite

and DIPEA in MeOH. This mixture was then passed through the second PFR at 50 °C, allowing for clean conversion of 3 to 2 in a 13 min residence time. Again, a mixing T-joint was used to merge this outgoing stream with a solution of PMEC phosphate 5 and DIPEA in MeOH for reaction in a final PFR at 60 °C with a 12.5 min residence time.

The outgoing stream of crude PIPN was monitored and maintained a steady-state concentration of ~80 mg/mL over the course of 3 h, ultimately allowing for the production of crude PIPN at a rate of ~25 g/h with this laboratory-scale setup. The use of online liquid chromatography sampling could be employed to monitor the composition of the various reaction streams exiting a PFR in order to ensure a consistent reaction profile.¹⁵

Crystallization of PIPN HBr was achieved by the addition of the crude reaction stream of PIPN and 2.5 equiv concentrated HBr into a seed bed of PIPN HBr in acetonitrile at 55 °C. Rapid desaturation was observed during the addition, and at the time of completion, the concentration of PIPN HBr was near-equilibrium solubility at 55 °C. This was followed by a controlled cooling of the batch temperature over 30 min and then a 1 h stir-out time to reach the near-equilibrium solubility of 8.5 mg/mL of PIPN HBr at 25 °C.¹² Conducting crystallization at elevated temperatures, followed by cooling to 25 °C, was found to offer increased robustness for the purity of isolated PIPN HBr from this process. With this continuous process, we were able to demonstrate the conversion of 1 to crude PIPN in just over 45 min of the total reaction time, streamlining the process by the removal of all aqueous workup and direct isolation by the addition of aqueous HBr to afford PIPN HBr 6 in 82% isolated yield with >99.9 LC area % purity on a >50 g scale. With the successful demonstration of a viable continuous process, we sought to further investigate the photochemical bromination in attempts to gain insights into

some of the more notable reaction features observed during our initial optimization.

Further Studies for Photochemical Bromination.

When considering the Wohl–Ziegler reaction, there are two mechanisms that have been the subject of much discussion in the literature (Figure 2). The Bloomfield mechanism, first

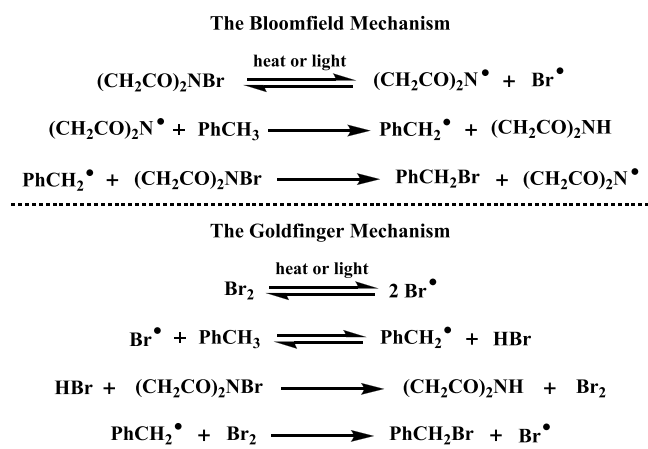


Figure 2. Bloomfield (top) and Goldfinger (bottom) mechanisms for the Wohl–Ziegler reaction.

proposed in 1944, postulates that NBS is the active brominating reagent and that the succinimidyl radical functions as the radical chain propagator.¹⁶ In the second mechanism, later proposed by Goldfinger, NBS serves to generate and maintain a low concentration of bromine throughout the course of the reaction, and the bromine radical functions as the radical chain propagator.¹⁷ Subsequent kinetic and mechanistic studies¹⁸ along with the demonstration that the N–Br^{19,20} bond dissociation energy is larger than that of the Br–Br¹⁸ have led to the Goldfinger mechanism being widely accepted as the operative mechanism in the Wohl–Ziegler reaction. However, this is not to say that finer points of the mechanism not depicted in Figure 2 do not play an important role. The existence of a radical-polarized transition state in the hydrogen atom abstraction event is supported by Hammett studies.²¹ Other considerations such as the formation of charge-transfer complexes²² and solvent cage interactions²³ have also been reported. Certainly, all these effects can have varying impacts on the overall transformation, depending on the exact reaction conditions employed, and the Wohl–Ziegler reaction remains as an intricate and fascinating reaction mechanism for study.

In our work, we noted several features of the photochemical bromination during our initial optimization reactions that prompted us to follow up with more detailed studies in order to further explore this transformation. Shown in Figure 3 is the reaction profile collected under our typical conditions for the bromination reaction 1 → 2 and 3. The top profile in Figure 3 tracks the consumption of 1 and the formation of 2 and 3. Of note was the induction period of approximately 60–90 s that was consistently observed when conducting the reaction under our standard photochemical conditions.²⁴ Clean conversion of 1 to 2 occurs over the first ~50% of the reaction, and the formation of dibromide 3 becomes more competitive as the reaction proceeds, highlighting the difficulty of driving this reaction to completion without the addition of excess NBS. The bottom profile in Figure 3 tracks the product (2 and 3)

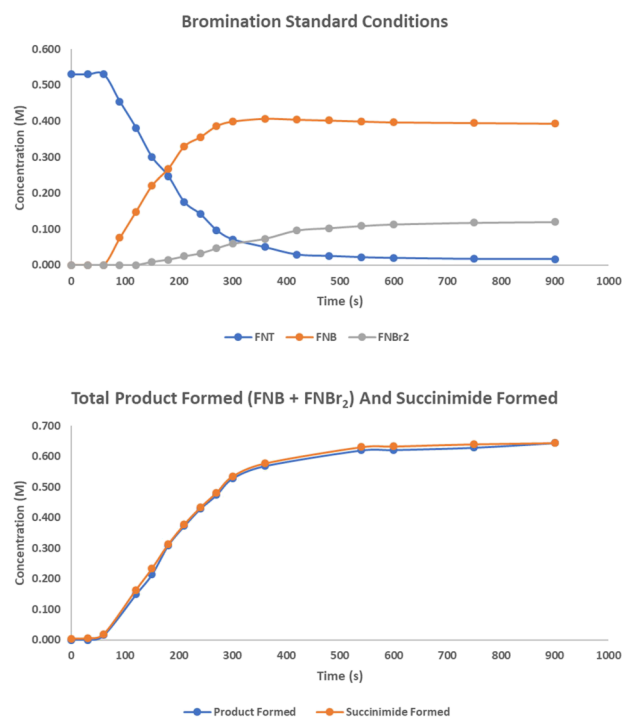


Figure 3. Conversion of 1 to 2 and 3 (top) and the overlay of total product and succinimide formed (bottom).

and succinimide formation. The close overlap of each indicates that NBS is turned over to succinimide as each bromination occurs and that there is no significant amount of excess bromine present throughout the course of the reaction.

The effects of residual bromine or HBr in NBS on the performance of Wohl–Ziegler reactions have been previously noted.^{4b,25} In line with the proposed Goldfinger mechanism, these small amounts of bromine or HBr could provide the initial low levels of bromine needed to initiate the reaction. We tested NBS from our commercial supplier (measured to contain 0.04 mol % bromine) and a recrystallized sample (measured to contain 0.03 mol % bromine), and in each case, identical reaction profiles for the bromination of 1 possessing an approximately 60–90 s induction was observed. This led us to believe that the very low levels of radical propagation species formed could be effectively quenched by residual oxygen during the induction period.²⁴ A control experiment monitoring the conversion of NBS to succinimide showed that during the induction period, an increase in the bromine concentration from an initial concentration of 0.12 mM up to 0.93 mM was observed after ~90 s (Figure 4 top). Conducting bromination with bromine levels spiked at 1 mM from the beginning showed a significant decrease in the induction period, while the conversion of 1 → 2 proceeded at the same rate as the standard reaction (Figure 4 bottom), indicating that the radical quenching of the induction period could be modulated by varying the initial bromine concentration. The effect of light intensity was also investigated. An increase in the light intensity (use of three LED rings instead of 1) reduced the time of the induction period but again had the same rate of reaction for the conversion of 1 → 2 (Figure 4 bottom). This suggests that under our standard conditions, after initiation, the reaction is saturated with respect to light, but it is not saturated during the process at work for generating the initial amount of bromine.²⁶

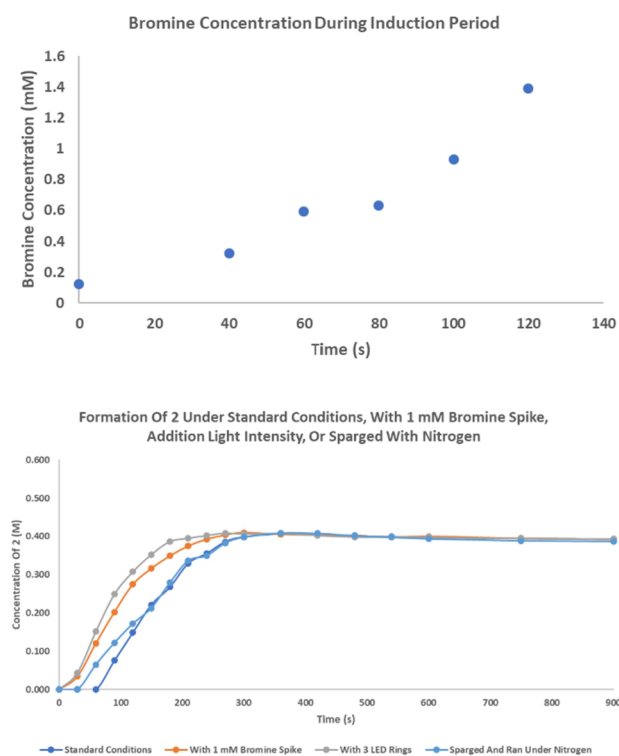


Figure 4. UV-vis assay of the bromine concentration during the conversion of NBS to succinimide (top). Comparison of standard reaction with reaction starting with 1 mM bromine concentration, a reaction with higher light intensity or with nitrogen-sparged solvent and ran under nitrogen (bottom).

Further experiments with higher charges of bromine concentrations at the beginning of the reaction by the addition of either 5 mol % bromine or 5 mol % HBr showed complete removal of the induction period and noticeably faster reaction rates. In order to confirm this is indeed a photochemically mediated process, we conducted an “on-off” experiment, where after ~50% conversion, the LED was turned off and the reaction was held at a temperature for 30 min, and then the LED was turned back on (Figure 5). Indeed, in the absence of

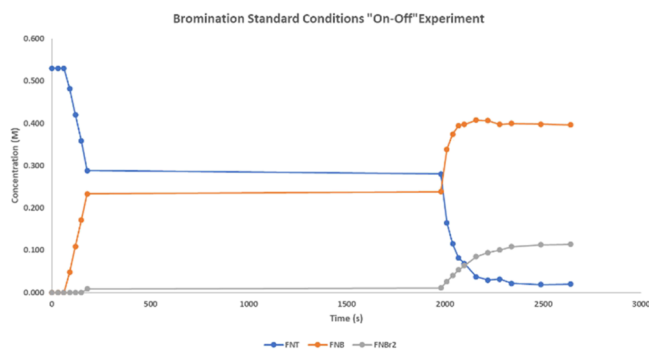


Figure 5. An “on-off” experiment for the bromination of **1**.

light, little reaction conversion (~1%) was observed, demonstrating the need for constant irradiation and that a thermal pathway for reaction did not contribute significantly to the overall transformation. Also, of note is that upon turning the LED on again, no induction period was observed, and the reaction progress proceeded at the same rate as when the LED

was first turned off, likely demonstrating that the low level of bromine persists in the reaction mixture.²⁷

Having investigated the role of bromine on the transformation, we then turned our attention toward kinetic studies through the use of reaction progress kinetic analysis (RPKA)²⁸ to further understand the influence that the concentrations TFA, NBS, and **1** have on the reaction profile. We began our studies by first performing different excess experiments with respect to TFA. When conducting the different excess TFA experiments under our standard conditions for bromination, we found identical reaction rates for the range tested from 1 to 25 mol % charges of TFA (Figure 6, top). The observed

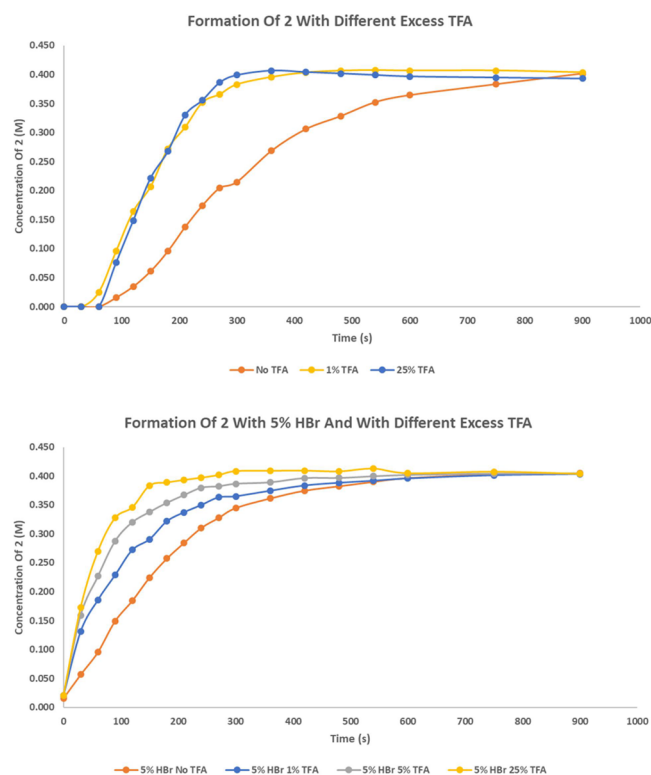


Figure 6. Reaction profile with no TFA, 1% TFA, and 25% TFA (top). Reaction profile with no TFA, 1% TFA, 5% TFA, and 25% TFA with 5% HBr added at the beginning of the reaction (bottom).

saturation kinetics indicate that a direct interaction between either **1** or NBS is not responsible for the rate acceleration that is seen with reactions containing TFA. It has been previously suggested that Brønsted acid additives in the Wohl-Ziegler reaction could offer rate acceleration by increasing the turnover of NBS to bromine.^{4b,29} While this is the case for the reaction of NBS with HBr, the saturation kinetics would imply that this is not the case for TFA. During the course of our studies, we have not observed any evidence of an interaction between TFA and NBS that would lead to the release of bromine, and the TFA concentration remains constant throughout the course of the reaction, indicating it is not being consumed through other pathways. Control experiments investigating the induction period showed no difference in the conversion of NBS to succinimide in the presence of TFA, and experiments monitoring the reaction of NBS with HBr to produce bromine and succinimide have shown that the reaction is very rapid and irreversible. Therefore, it is unlikely that the rate acceleration would be attributed to the participation of TFA in the process

to turn over NBS to bromine.¹² The saturation kinetics observed suggest that TFA may be interacting with a species present in only relatively low levels during the course of the reaction, possibly either with bromine or a bromine radical. With this in mind, a second set of different excess experiments were conducted with a 5 mol % spike of HBr at the beginning of the reaction, ensuring that a relatively large amount of bromine would be present throughout the course of the reaction as compared to our standard conditions. In this case, a very clear trend showing rate acceleration was observed for each different charge of TFA at 1, 5, and 25 mol %. The observed response under these conditions offers some evidence for an interaction between TFA and either bromine or a bromine radical that could be responsible for the rate acceleration.

With the RPKA completed for TFA, we moved to explore different excess experiments with respect to **1** and NBS. Throughout the course of our optimization and initial kinetic studies, we had relied on aliquot and time point analysis for monitoring reaction progress, which was often labor-intensive and required the preparation of multiple samples for analysis. This also limited the data point resolution we could obtain, which made more subtle aspects difficult to capture. A particularly attractive technique developed in recent years for continuous monitoring of photochemical reactions by nuclear magnetic resonance (NMR) offers a convenient solution to these issues.³⁰ In this case, reaction progress could be monitored by NMR on a single sample with a fiber optic cable inserted into the NMR tube for irradiation, and data could be collected with high temporal resolution (~5 to 10 s). We found that this technique was particularly useful when collecting data for RPKA work with **1** and NBS and processing by either the initial rate or variable time normalization analysis (VTNA).^{12,31} A standard reaction profile collected using this technique is shown in Figure 7 (top) monitoring reaction progress by ¹⁹F NMR, which was especially useful in this case for tracking TFA as well. The reaction profile is in line with our earlier analysis, but with much higher data density now. This allowed for the collection of data for the different excess experiments with respect to **1** and NBS with the resolution needed for the initial rate and VTNA processing at the standard reaction conditions. Pictured in Figure 7 (middle) is the overlay for the formation of **2** for the different excess experiments of **1** and NBS without TFA present. In each different excess experiment, the concentration of **2** or NBS was half of the standard concentration. The clear overlay of these two different excess experiments indicates the same reaction order with respect to either **1** or NBS, and initial rate or VTNA processing both show first-order reaction dependence with respect to each component. However, this is not the case when conducting the analogous different excess experiments with TFA present. In this case, the overlay is not the same, and a first-order reaction dependence is still observed for NBS, but the reaction order for **2** is now closer to 0.5.¹² The same reaction order observed with respect to NBS both in the presence and absence of TFA is in agreement with our earlier observations that there does not appear to be a direct interaction of TFA and NBS under the reaction conditions. The different reaction order seen for **1**, however, suggests that there is some interaction with TFA during the course of the reaction. Taking this into account along with the dependence on the bromine concentration also effecting the rate of the reaction, this may be an indication that TFA could play a role

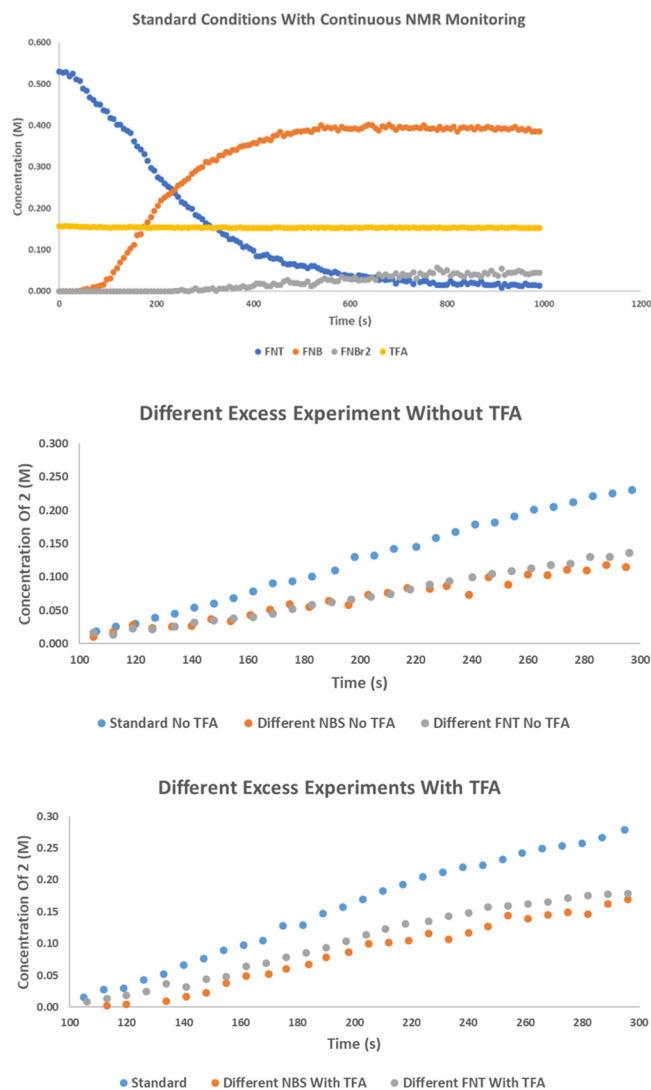


Figure 7. Standard reaction with continuous monitoring by NMR (top). Different excess experiments for **1** and NBS without TFA (middle). Different excess experiments for **1** and NBS with TFA (bottom).

in assisting with the hydrogen atom abstraction event, which is believed to be the rate-determining step in this reaction.²⁵ The fractional order with respect to **1** may also be an indication that multiple reaction pathways for the conversion of **1** to **2** and **3** could occur competitively that may or may not involve TFA. While the exact nature of the role TFA in this reaction is not fully understood at the point, we believe the studies here offer insights helpful for further probing the complexity and fascinating aspects of the Wohl–Ziegler reaction.

CONCLUSIONS

In conclusion, we have reported our development work on photochemical bromination and demonstrated the utility in a continuous process for the preparation of **6** en route to AMG 423. This continuous process offered several distinct advantages over the current process in that it offers significantly shorter reaction times, reduced waste by eliminating all aqueous work ups, and allowed for direct crystallization from the crude reaction mixture. This process was demonstrated in laboratory-scale runs to produce crude

PIPn at rates up to 25 g/h with a total residence time from the beginning to the end of approximately 45 min. Detailed kinetic studies offered insights into key features of the reaction, such as the concentration and the role of bromine in these reactions and the effects of TFA as an additive in this transformation. These kinetic studies coupled with the use of continuous monitoring by NMR offers a powerful technique for the characterization and further development of reactions of this type and will no doubt be a valuable resource in future development work.

EXPERIMENTAL SECTION

General Materials and Methods. Photochemical reactions were conducted under an ambient atmosphere, while all other transformations were conducted under a nitrogen atmosphere using anhydrous solvents. All commercially obtained reagents were used as received. A kit from Sigma-Aldrich for a LED microphotochemical reactor was used for reaction development, and the equipment for photoNMR experiments was purchased from Goldstone Scientific (see the [Supporting Information](#) for more details). Experiments for reaction screening and kinetics were conducted in 1-dram vials or NMR tubes. Other batch experiment work was conducted in Mettler-Toledo EasyMax reactors. PFRs for laboratory-scale experiment were constructed from 1/8" ID, 1/4" OD PFA tubing. ^1H NMR spectra were recorded on Bruker spectrometers (at 400 MHz) and are reported relative to deuterated solvent signals (7.27 ppm for CDCl_3 and 2.50 ppm for $\text{DMSO-}d_6$). Data for ^1H NMR spectra are reported as follows: chemical shift (δ ppm), multiplicity, coupling constant (Hz), and integration.

General Procedure for Photochemical Bromination. A 10 mL volumetric flask is charged with **1** (822 mg, 5.30 mmol, 1 equiv), followed by the addition of 6 mL of acetonitrile (or d_3 -acetonitrile for NMR experiments). Then, NBS (1.18 g, 6.63 mmol, 1.25 equiv) and TFA (151 mg, 0.099 mL, 1.33 mmol, 0.25 equiv) were charged to the volumetric flask, followed by the appropriate amount of acetonitrile (or d_3 -acetonitrile for NMR experiments) to bring the final volume to 10 mL (530 mM concentration with respect to **1**). For experiments using 1-dram vials, 2.8 mL of this solution is dispensed into the vial, and for experiments using an NMR tube, 0.5 mL of this solution is dispensed into the NMR tube. The reaction vessel is then placed in a water bath heated to 80 °C and irradiated for 15 min to furnish a mixture of **1** (3% assay yield), **2** (74% assay yield), and **3** (23% assay yield).

Procedure for the Continuous Process. A 2 L Schott bottle is charged with acetonitrile (1087 mL), followed by the addition of **1** (100 g, 647 mmol, 1 equiv), NBS (144 g, 806 mmol, 1.25 equiv), and TFA (18.4 g, 12.0 mL, 161 mmol, 0.25 equiv).

A second 250 mL Schott bottle is charged with methanol (100 mL) followed by the addition of diethyl phosphite (33.2 mL, 258 mmol, 0.4 equiv) and DIPEA (73 mL, 419 mmol, 0.65 equiv).

A third Schott bottle was charged with methanol (300 mL), followed by **5** (144 g, 648 mmol, 1 equiv) and DIPEA (281 mL, 1611 mmol, 2.5 equiv). The mixture was filtered through a pad of Celite and then washed with methanol (170 mL). The combined filtrate was transferred back to the Schott bottle.

As depicted in [Figure 1](#), the acetonitrile solution of **1**, NBS, and TFA was then pumped through a coiled tube PFR (1/8" ID, 1/4" OD PFA tubing) irradiated under 435–445 nm LEDs

(in this case, a stack of 4 LEDs was used to cover the length of the PFR at a distance of 3 cm) and submerged in a thermostated water bath maintained at 77 °C at a rate of 2.9 mL/min (total residence time of 20 min). This stream was then joined together with the stream of diethyl phosphite and DIPEA in methanol pumped at 0.46 mL/min at a T-mixer joint. The outgoing combined stream was then pumped through a coiled tube PFR submerged in a thermostated water bath maintained at 50 °C at a rate of 3.36 mL/min (total residence time of 13 min). Finally, this stream was then joined together with the stream of **5** and DIPEA in methanol pumped at 1.65 mL/min at a T-mixer joint. The outgoing combined stream was then pumped through a coiled tube PFR submerged in a thermostated water bath maintained at 60 °C at a rate of 5.01 mL/min (total residence time of 12.5 min). The resulting crude stream of PIPn was collected in a Schott bottle at 25 °C.

A seed bed of **6** was then prepared by charging a 1 L jacketed reactor with acetonitrile (80 mL) and **6** (1.4 g) and heating the batch to 55 °C. To the seed bed was then added simultaneously 590 mL of the crude PIPn solution (concentration 82.2 mg/mL of crude PIPn, 48.5 g, 163 mmol) at a rate of 300 mL/h and concentrated HBr (48 wt/wt %, 45.6 mL, 408 mmol, 2.5 equiv relative to crude PIPn) at a rate of 22.8 mL/h. The batch was then cooled to 25 °C over 30 min followed by addition stir out at 25 °C for 1 h. The mixture was then filtered, and the cake was washed with 3 × 100 mL of acetonitrile washings at 55 °C. After drying, 50.7 g of **6** was obtained as a white solid for an overall of 82% yield.

Fluoro-Nitrotoluene 1. ^1H NMR (400 MHz, CDCl_3) δ 7.89–7.80 (m, 1H), 7.52–7.43 (m, 1H), 7.89–7.80 (m, 1H), 2.39 (d, $J = 4.0$ Hz, 3H).³²

Monobromide 2. ^1H NMR (400 MHz, CDCl_3) δ 8.07–7.97 (m, 1H), 7.77–7.67 (m, 1H), 7.35–7.27 (m, 1H), 4.56 (s, 2H).³⁰

Dibromide 3. ^1H NMR (400 MHz, CDCl_3): δ 8.23–8.14 (m, 1H), 8.09–8.02 (m, 1H), 7.46–7.38 (m, 1H), 6.97 (s, 1H).³⁰

PIPn HBr 6. ^1H NMR (400 MHz, $\text{DMSO-}d_6$) δ 11.74 (br s, 1H), 8.30–8.22 (m, 1H), 8.22–8.10 (m, 1H), 7.54 (t, $J = 8$ Hz, 1H), 4.45 (br s, 2H), 4.02 (br s, 2H), 3.63 (s, 3H), 3.44 (br s, 4H), 3.11 (br s, 2H).³³

ASSOCIATED CONTENT

Supporting Information

The Supporting Information is available free of charge at <https://pubs.acs.org/doi/10.1021/acs.oprd.1c00469>.

Experimental procedures, characterization data, reaction optimization data, reaction setup details, and kinetic data ([PDF](#))

AUTHOR INFORMATION

Corresponding Author

Kyle Quasdorf – Pivotal and Commercial Drug Substance Technologies, Process Development, Amgen Inc., Thousand Oaks, California 91320, United States; orcid.org/0000-0003-0151-6511; Email: quasdorf@amgen.com

Authors

James I. Murray – Pivotal and Commercial Drug Substance Technologies, Process Development, Amgen Inc., Thousand Oaks, California 91320, United States

- Hanh Nguyen – Pivotal and Commercial Drug Substance Technologies, Process Development, Amgen Inc., Thousand Oaks, California 91320, United States
- Maria V. Silva Elipe – Attribute Sciences Department, Amgen Inc., Thousand Oaks, California 91320, United States; orcid.org/0000-0002-8429-9534
- Ari Ericson – Pivotal and Commercial Drug Substance Technologies, Process Development, Amgen Inc., Thousand Oaks, California 91320, United States
- Eric Kircher – Attribute Sciences Department, Amgen Inc., Thousand Oaks, California 91320, United States
- Lianxiu Guan – Attribute Sciences Department, Amgen Inc., Thousand Oaks, California 91320, United States
- Seb Caille – Pivotal and Commercial Drug Substance Technologies, Process Development, Amgen Inc., Thousand Oaks, California 91320, United States; orcid.org/0000-0001-5434-5483

Complete contact information is available at:
<https://pubs.acs.org/10.1021/acs.oprd.1c00469>

Notes

The authors declare no competing financial interest.

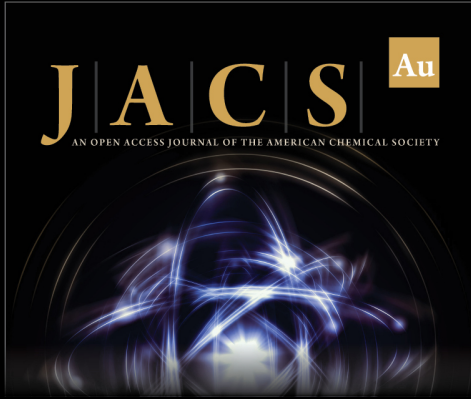
ACKNOWLEDGMENTS

We acknowledge Dr. Adam Simon and Professor Tehshik Yoon for insightful discussions related to this work.

REFERENCES

- (1) (a) Wohl, A. Bromierung ungesättigter Verbindungen mit N-Brom-acetamid, ein Beitrag zur Lehre vom Verlauf chemischer Vorgänge. *Ber. Dtsch. Chem. Ges.* **1919**, *52*, 51–63. (b) Ziegler, K.; Späth, A.; Schaaf, E.; Schumann, W.; Winkelmann, E. Die Halogenierung ungesättigter Substanzen in der Allylstellung. *Liebigs Ann. Chem.* **1942**, *551*, 80–119. (c) Djerassi, C. Brominations with N-Bromosuccinimide and Related Compounds. The Wohl-Ziegler Reaction. *Chem. Rev.* **1948**, *43*, 271–317. (d) Saikia, I.; Borah, A. J.; Phukan, P. Use of Bromine and Bromo-Organic Compounds in Organic Synthesis. *Chem. Rev.* **2016**, *116*, 6837–7042.
- (2) Murray, J. I.; Silva Elipe, M. V.; Cosbie, A.; Baucom, K.; Quasdorf, K.; Caille, S. Kinetic Investigations To Enable Development of a Robust Radical Benzylic Bromination for Commercial Manufacturing of AMG 423 Dihydrochloride Hydrate. *Org. Process Res. Dev.* **2020**, *24*, 1523–1530.
- (3) Caille, S.; Allgeier, A. M.; Bernard, C.; Correll, T. L.; Cosbie, A.; Crockett, R. D.; Cui, S.; Faul, M. M.; Hansen, K. B.; Huggins, S.; Langille, N.; Mennen, S. M.; Morgan, B. P.; Morrison, H.; Muci, A.; Nagapudi, K.; Quasdorf, K.; Ranganathan, K.; Roosen, P.; Shi, X.; Thiel, O. R.; Wang, F.; Tvetan, J. T.; Woo, J. C. S.; Wu, S.; Walker, S. D. Development of a Factory Process for Omecamtiv Mecarbil, a Novel Cardiac Myosin Activator. *Org. Process Res. Dev.* **2019**, *23*, 1558–1567.
- (4) (a) Cantillo, D.; de Frutos, O.; Rincon, J. A.; Mateos, C.; Kappe, C. O. A Scalable Procedure for Light-Induced Benzylic Brominations in Continuous Flow. *J. Org. Chem.* **2014**, *79*, 223–229. (b) Bonfield, H. E.; Williams, J. D.; Ooi, W. X.; Leach, S. G.; Kerr, W. J.; Edwards, L. J. A Detailed Study of Irradiation Requirements Towards an Efficient Photochemical Wohl-Ziegler Procedure in Flow. *ChemPhotoChem* **2018**, *2*, 938–944. (c) Zhao, M.; Li, M.; Lu, W. Visible-Light-Driven Oxidative Mono- and Dibromination of Benzylic sp³ C–H Bonds with Potassium Bromide/Oxone at Room Temperature. *Synthesis* **2018**, *50*, 4933–4939. (d) Chen, Y.; de Frutos, O.; Mateos, C.; Rincon, J. A.; Cantillo, D.; Kappe, C. O. Continuous Flow Photochemical Benzylic Bromination of a Key Intermediate in the Synthesis of a 2-Oxazolidinone. *ChemPhotoChem* **2018**, *2*, 906–912. (e) Steiner, A.; Roth, P. M. C.; Strauss, F. J.; Gauron, G.; Tekautz, G.; Winter, M.; Williams, J. D.; Kappe, C. O. Multikilogram per Hour Continuous Photochemical Benzylic Brominations Applying a Smart Dimensioning Scale-up Strategy. *Org. Process Res. Dev.* **2020**, *24*, 2208–2216.
- (5) (a) Ji, Y.; Bottecchia, C.; Lévesque, F.; Narsimhan, K.; Lehnerr, D.; McMullen, J. P.; Dalby, S. M.; Xiao, K.-J.; Reibarkh, M. Benzylic Photobromination for the Synthesis of Belzutifan: Elucidation of Reaction Mechanisms Using In Situ LED-NMR. *J. Org. Chem.* **2021**, DOI: [10.1021/acs.joc.1c01465](https://doi.org/10.1021/acs.joc.1c01465). (b) Bottecchia, C.; Lévesque, F.; McMullen, J. P.; Ji, Y.; Reibarkh, M.; Peng, F.; Tan, L.; Spencer, G.; Nappi, J.; Lehnerr, D.; Narsimhan, K.; Wismer, M. K.; Chen, L.; Lin, Y.; Dalby, S. M. Manufacturing Process Development for Belzutifan, Part 2: A Continuous Flow Visible-Light-Induced Benzylic Bromination. *Org. Process Res. Dev.* **2021**, DOI: [10.1021/acs.oprd.1c00240](https://doi.org/10.1021/acs.oprd.1c00240).
- (6) (a) Su, Y.; Straathof, N. J. W.; Hessel, V.; Noël, T. Photochemical Transformations Accelerated in Continuous-Flow Reactors: Basic Concepts and Applications. *Chem. – Eur. J.* **2014**, *20*, 10562–10589. (b) Cantillo, D.; Kappe, C. O. Halogenation of organic compounds using continuous flow and microreactor technology. *React. Chem. Eng.* **2017**, *2*, 7–19. (c) Šterk, D.; Jukič, M.; Časar, Z. Application of Flow Photochemical Bromination in the Synthesis of a 5-Bromomethylpyrimidine Precursor of Rosuvastatin: Improvement of Productivity and Product Purity. *Org. Process Res. Dev.* **2013**, *17*, 145–151.
- (7) A kit from Sigma-Aldrich for a LED micro photochemical reactor was used for reaction development. See SI for more details.
- (8) A material of construction compatibility assessment should be conducted for any process using concentrated HBr.
- (9) (a) İçten, E.; Maloney, A. J.; Beaver, M. G.; Shen, D. E.; Zhu, X.; Graham, L. R.; Robinson, J. A.; Huggins, S.; Allian, A.; Hart, R.; Walker, S. D.; Rolandi, P.; Braatz, R. D. A Virtual Plant for Integrated Continuous Manufacturing of a Carfilzomib Drug Substance Intermediate, Part 1: CDI-Promoted Amide Bond Formation. *Org. Process Res. Dev.* **2020**, *24*, 1861–1875. (b) İçten, E.; Maloney, A. J.; Beaver, M. G.; Zhu, X.; Shen, D. E.; Robinson, J. A.; Parson, A. T.; Allian, A.; Huggins, S.; Hart, R.; Rolandi, P.; Walker, S. D.; Braatz, R. D. A Virtual Plant for Integrated Continuous Manufacturing of a Carfilzomib Drug Substance Intermediate, Part 2: Enone Synthesis via a Barbier-Type Grignard Process. *Org. Process Res. Dev.* **2020**, *24*, 1876–1890. (c) Maloney, A. J.; İçten, E.; Capellades, G.; Beaver, M. G.; Zhu, X.; Graham, L. R.; Brown, D. B.; Griffin, D. J.; Sangodkar, R.; Allian, A.; Huggins, S.; Hart, R.; Rolandi, P.; Walker, S. D.; Braatz, R. D. A Virtual Plant for Integrated Continuous Manufacturing of a Carfilzomib Drug Substance Intermediate, Part 3: Manganese-Catalyzed Asymmetric Epoxidation, Crystallization, and Filtration. *Org. Process Res. Dev.* **2020**, *24*, 1891–1908. (d) Beaver, M. G.; Shi, X.; Riedel, J.; Patel, P.; Zeng, A.; Corbett, M. T.; Robinson, J. A.; Parsons, A. T.; Cui, S.; Baucom, K.; Lovette, M. A.; İçten, E.; Brown, D. B.; Allian, A.; Flick, T. G.; Chen, W.; Yang, N.; Walker, S. D. Continuous Process Improvement in the Manufacture of Carfilzomib, Part 2: An Improved Process for Synthesis of the Epoxyketone Warhead. *Org. Process Res. Dev.* **2020**, *24*, 490–499.
- (10) Beaver, M. G.; Zhang, E.-X.; Liu, Z.-Q.; Zheng, S.-Y.; Wang, B.; Lu, J.-P.; Tao, J.; Gonzalez, M.; Jones, S.; Tedrow, J. S. Development and Execution of a Production-Scale Continuous [2 + 2] Photocycloaddition. *Org. Process Res. Dev.* **2020**, *24*, 2139–2146.
- (11) Tom, J. K.; Achmatowicz, M. M.; Beaver, M. G.; Colyer, J.; Ericson, A.; Hwang, T.-L.; Jiao, N.; Langille, N. F.; Liu, M.; Lovette, M. A.; Sangodkar, R. P.; Kumar, S. S.; Spada, S.; Perera, D.; Sheeran, J.; Campbell, K.; Doherty, T.; Ford, D. D.; Fang, Y.-Q.; Rossi, E.; Santoni, G.; Cui, S.; Walker, S. D. Implementing Continuous Manufacturing for the Final Methylation Step in the AMG 397 Process to Deliver Key Quality Attributes. *Org. Process Res. Dev.* **2021**, *25*, 486–499.
- (12) See SI for further experimental details.
- (13) In Figure 1 the abbreviation V represents volumes and it equals liters of solvent per kilogram of 1.
- (14) Note: The bromination mixture is incompatible with metal and metal components should be avoided at and before the first PFR.

- (15) Malig, T. C.; Koenig, J. D. B.; Situ, H.; Chehal, N. K.; Hultin, P. G.; Hein, J. E. Time HPLC-MS Reaction Progress Monitoring Using an Automated Analytical Platform. *React. Chem. Eng.* **2017**, *2*, 309–314.
- (16) Bloomfield, G. F. Rubber, polyisoprenes, and allied compounds. Part VI. The mechanism of halogen-substitution reactions, and the additive halogenation of rubber and of dihydromyrcene. *J. Chem. Soc.* **1944**, 114–120.
- (17) Adam, J.; Gosselain, P. A.; Goldfinger, P. Laws of Addition and Substitution in Atomic Reactions of Halogens. *Nature* **1953**, *171*, 704–705.
- (18) (a) Pearson, R. E.; Martin, J. C. The mechanism of benzylic bromination with N-bromosuccinimide. *J. Am. Chem. Soc.* **1963**, *85*, 354–355. (b) Russell, G. A.; DeBoer, C.; Desmond, K. M. Mechanisms of Benzylic Bromination. *J. Am. Chem. Soc.* **1963**, *85*, 365–366. (c) Day, J. C.; Lindstrom, M. J.; Skell, P. S. Succinimidyl radical as a chain carrier. Mechanism of allylic bromination. *J. Am. Chem. Soc.* **1974**, *96*, 5616–5617.
- (19) O'Reilly, R. J.; Karton, A. A dataset of highly accurate homolytic N–Br bond dissociation energies obtained by Means of W2 theory. *Int. J. Quantum Chem.* **2016**, *116*, 52–60.
- (20) Luo, Y. R. *Comprehensive Handbook of Chemical Bond Energies*; CRC Press, 2007.
- (21) (a) Kim, S. S.; Choi, S. Y.; Kang, C. H. The reality of polar transition states of photobromination of toluenes by N-bromosuccinimide (NBS). *J. Am. Chem. Soc.* **1985**, *107*, 4234–4237. (b) Kim, S. S.; Lee, C. S.; Kim, C. C.; Kim, H. J. Negligible kinetic solvent interactions for the rate of photobromination of toluenes where the bromine atom is a principal chain carrier. *J. Phys. Org. Chem.* **1990**, *3*, 803–806.
- (22) (a) Yamamoto, N.; Kajikawa, T.; Sato, H.; Tsubomura, H. Charge-transfer spectra of halogen atoms and the halogenation reaction of aromatics studies by the flash technique. *J. Am. Chem. Soc.* **1969**, *91*, 265–267. (b) Bunce, N. J.; Ingold, K. U.; Landers, J. P.; Luszyk, J.; Scaiano, J. C. Kinetic study of the photochlorination of 2,3-dimethylbutane and other alkanes in solution in the presence of benzene. First measurements of the absolute rate constants for hydrogen abstraction by the "free" chlorine atom and the chlorine atom-benzene pi-complex. Identification of these two species as the only hydrogen abstractors in these systems. *J. Am. Chem. Soc.* **1985**, *107*, 5464–5472.
- (23) Tanner, D. D.; Meintzer, C. P.; Tsai, E. C.; Oumar-Mahamat, H. Cage return and solvent viscosity. Effect of viscosity on polar effects inherent in benzylic bromination. *J. Am. Chem. Soc.* **1990**, *112*, 7369–7372.
- (24) The impact of oxygen on induction periods was noted by Goldfinger early studies see Goldfinger, P.; Gosselain, P. A.; Martion, R. H. Induction Periods in Reactions of N-Halogenimides. *Nature* **1951**, *168*, 30–32. In our work described here all reactions were conducted under ambient atmosphere. A control experiment conducted under nitrogen atmosphere with nitrogen sparged solvent showed a slightly reduced induction period but the same reaction rate for the bromination of **1** (Figure 4). Reference 4b also observes a similar induction period for these types of reactions
- (25) Dauben, H. J.; McCoy, L. L. N-Bromosuccinimide. I. Allylic Bromination, a General Survey of Reaction Variables. *J. Am. Chem. Soc.* **1959**, *81*, 4863–4873.
- (26) Lu, F. L.; Naguib, Y. M. A.; Kitadani, M.; Chow, Y. L. An investigation of the photodecomposition of N-bromosuccinimide; the generation and reactivity of succinimidyl radical. *J. Can. J. Chem.* **1979**, *57*, 1967–1976.
- (27) For studies on termination steps in radical brominations see Verwater, H. J. C.; van Beek, H. C. A. Kinetics and mechanism off the radical chain photobromination of toluene. *Ind. Eng. Chem. Prod. Res. Dev.* **1986**, *25*, 631–633.
- (28) Blackmond, D. G. Reaction Progress Kinetic Analysis: A Powerful Methodology for Mechanistic Studies of Complex Catalytic Reactions. *Angew. Chem., Int. Ed.* **2005**, *44*, 4302–4320.
- (29) Offermann, W.; Vögtle, F. Side Chain Brominations by N-Bromosuccinimide; IV. Novel and Improved Preparations by Selective Choice of Solvents. *Synthesis* **1977**, *4*, 272–273.
- (30) (a) Feldmeier, C.; Bartling, H.; Riedle, E.; Gschwind, R. M. LED based NMR illumination device for mechanistic studies on photochemical reactions – Versatile and simple, yet surprisingly powerful. *J. Magn. Reson.* **2013**, *232*, 39–44. (b) Ji, Y.; DiRocco, D. A.; Kind, J.; Thiele, C. M.; Gschwind, R. M.; Reibarkh, M. LED-Illuminated NMR Spectroscopy: A Practical Tool for Mechanistic Studies of Photochemical Reactions. *ChemPhotoChem* **2019**, *3*, 984–992. (c) Lehnerr, D.; Ji, Y.; Neel, A. J.; Cohen, R. D.; Brunskill, A. P. J.; Yang, J.; Reibarkh, M. Discovery of a Photoinduced Dark Catalytic Cycle Using *in Situ* LED-NMR Spectroscopy. *J. Am. Chem. Soc.* **2018**, *140*, 13843–13853. (d) Ji, Y.; DiRocco, D. A.; Hong, C. M.; Wismer, M. K.; Reibarkh, M. Facile Quantum Yield Determination via NMR Actinometry. *Org. Lett.* **2018**, *20*, 2156–2159.
- (31) Burés, J. A Simple Graphical Method to Determine the Order in Catalyst. *Angew. Chem., Int. Ed.* **2016**, *55*, 16084–16087.
- (32) ¹H NMR matches characterization previously reported in ref 2.
- (33) PIPN HCl salt characterized previously in ref 3.



Editor-in-Chief
Prof. Christopher W. Jones
Georgia Institute of Technology, USA

Open for Submissions 

pubs.acs.org/jacsau  ACS Publications
Most Trusted. Most Cited. Most Read.